

A comparison of fill factor and recombination losses in amorphous silicon solar cells on ZnO and SnO₂

A. Alkaya^a, R. Kaplan^{b,*}, H. Canbolat^a, S.S. Hegedus^c

^a Department of Electrical-Electronics Engineering, University of Mersin, Ciftlikkoy Campus, 33343 Mersin, Turkey

^b Department of Secondary Science and Mathematics Education, University of Mersin, Yenisehir Campus, 33169 Mersin, Turkey

^c Institute of Energy Conversion, University of Delaware, Newark, DE 19716, USA

ARTICLE INFO

Article history:

Received 29 June 2007

Accepted 12 November 2008

Available online 6 December 2008

Pacs:

77.20.Jv

72.80.Ng

73.50.Pz

Keywords:

ZnO and SnO₂/a-Si:H p-i-n solar cell

Fill factor

Quantum efficiency

Intensity- and frequency-dependence of

photocurrent

Recombination

ABSTRACT

Effects of ZnO and SnO₂ TCO (Transparent Conductive Oxide) substrate materials on hydrogenated amorphous silicon (a-Si:H) p-i-n solar cell performances and recombination kinetics have been investigated. DC and Frequency-resolved photocurrent measurements in a-Si:H p-i-n solar cells of 6 have been carried out experimentally. In particular, the *I*-*V* characteristics in the dark and light, the quantum efficiency spectra, the intensity-, bias voltage- and frequency-dependence of photocurrent were obtained. Fill factor (FF) values were determined from *I*-*V* characteristics for both types of substrate cells under various illumination levels. The exponent ν in the power-law relationship, $I_{ph} \propto G^\nu$, between generating flux density and photocurrent were determined at different bias voltages (DC) and modulation frequencies. High values of V_{oc} (open-circuit voltage), FF, and DC exponent ν for the a-Si:H p-i-n solar cell with SnO₂ were obtained, but the integrated QE (quantum efficiency), the modulated exponent ν were found to be low compared to cells prepared on ZnO substrates. Our results show that these parameters are sensitive to the ZnO and SnO₂ substrate materials which act as a window layer allowing most of the incident light to pass into the i-layer of p-i-n cells.

© 2008 Elsevier Ltd. All rights reserved.

1. Introduction

In recent years electricity generation from renewable resources has been counted upon to bridge the gap between global demand and supply of power. Solar has good potential and the direct conversion technology based on solar photovoltaics has several positive attributes [1–3].

The hydrogenated amorphous silicon (a-Si:H) p-i-n thin film has been the most promising material in the photovoltaic application, especially for the solar cell with low cost and a large area [4,5]. However, the light induced degradation [6], is the major obstacle for a-Si:H to be used in solar cell application. The performance of the solar cell was characterized by the *I*-*V* curves, the frequency- and intensity-dependent photocurrent, and the spectral photoresponse. The spectral photoresponse and thus the quantum efficiency have been used to characterize the ability to collect charge carriers generated by different wavelengths of the sun spectrum, which are powerful tools for the development and calibration of solar cells, due to the fact that the light is absorbed

differently in each layer, and it allows monitoring the layers' properties.

The main research activities in the photovoltaic field are related to materials development, which can be obtained at relatively low cost and to improve the conversion efficiency [7,8]. One of the known ways to increase the conversion efficiency is the reducing of the radiation losses at the front surface of the cell. For a-Si:H TCO/p-i-n solar cells, minimizing the resistance between the p-layer and TCO is critical issue for utilizing new TCO materials like ZnO. However, characterization of the TCO/p interface is difficult since it is in series with dominant p-i-n junction [9].

It is well-known that although textured SnO₂:F is the industry Standard for superstrate (glass/TCO/p-i-n/metal) type a-Si solar cells, it has two weaknesses. First, SnO₂ is chemically reduced by H or SiH₄ plasma which leaves a thin layer of Sn which reduces its transmission. Second, SnO₂ has only about 93–95% internal transmission over the visible spectrum. In comparison, textured ZnO has been shown to be plasma resistant and to have 96–97% transmission over the visible spectrum [10]. However, electrical performance of ZnO/p-i-n cells is generally poorer than SnO₂/p-i-n cells. It is nearly found that devices deposited on textured ZnO tend to have lower FF and V_{oc} . Recent analysis of devices indicates lower V_{oc} and

* Corresponding author. Tel.: +90 324 3412815x2021; fax: +90 324 3412823.
E-mail address: ruhikaplan@yahoo.com (R. Kaplan).

FF observed with ZnO is not due to the contact but to changes in the p/i junction recombination [9].

Charge carrier transport underlies the electrical behaviour of any semiconductor device and, in particular, of solar cells. Despite the efforts made to correctly model such transport in semiconductors over the years, many questions still remain open.

The aim of this paper is to optimize the radiation and recombination losses by investigating two types of p-i-n solar cells which have the same a-Si recipe and back contact but different ZnO and SnO₂ TCO substrate materials.

2. Experimental details

In this work, we used 6 of samples which are 1 × 1 in. substrates of a-Si:H p-i-n devices. These devices were obtained from The IEC Lab of Delaware University. The cells have a layer-sequence of glass/TCO/p-i-n/TiAg. The substrate material (TCO) used in the cell structure and *J-V* results were given in Table 1. These measurements were taken under ~1 sun illumination by using 4-terminal configuration due to the high resistance. All cells have the same a-Si device deposition conditions and back contact (Ti/Ag). The differences are with the TCO substrates. The ZnO are made by APCVD by Roy Gordon's group at Harvard (HRVD). LOF is Libbey-Owen-Ford SnO₂ less textured than Solarex. SLX is Solarex SnO₂. The area is 0.4 cm² for all cells, and the substrate contact is along the side. The i-layer thickness is about 0.5–0.6 μm for all devices. The transmission of all of the samples was about 92–93% for wavelengths higher than 600 nm, assuming a value of 100% for the transmission of the glass substrate. The average haze ratios are 0.09 and 0.03 for high- and low-textured TCO respectively [11]. Our TCO materials used have a sufficiently high value of electrical conductivity, i.e., a low electrical resistivity (about 1 Ω cm²) [9].

An HeNe laser (632.8 nm, 0.65 mm beam diameter, 10 mW o/p max.) was used as the excitation light to obtain *I-V* characteristics, intensity- and frequency-dependences of photocurrent. Neutral density filters (NDF) were used to vary the intensity of light incident on the p-i-n solar cell to between 20 μW and 10 mW. The incident light was chopped at the frequencies between 10 Hz and 4 kHz. The modulated signals were detected by pre- and lock-in amplifiers. For DC measurements, an electrometer (Model 6514) was used.

The quantum efficiency (QE) was measured from 400 to 750 nm using the same lock-in detection system chopped at 70 Hz, illuminated through a monochromator having 12 nm width at half maximum. The system was calibrated using a filtered (Schott KG5) crystalline Si device as was used to calibrate the Oriel solar simulator.

The only best results for solar cells on ZnO and SnO₂ (Table 1) were reported in the following. All results were obtained at room temperature.

3. Results and discussion

The electrical performance of a solar cell is described by the relation between the current density *J* (= *I/A*, where *I* current, *A*

area) flowing through the cell and the potential *V* across it, while the cell is illuminated. A convenient way to characterize the electrical performance of a solar cell is to specify its open-circuit voltage *V*_{oc}, its short-circuit current density *J*_{sc} and its fill factor FF. The latter is a measure of the rectangularity of the *J-V* curve and is defined by

$$FF = (V_m J_m) / (V_{oc} J_{sc}) \quad (1)$$

where *V*_m and *J*_m are the voltage and current density at the maximum power point respectively, and (*V*_m*J*_m) is the maximum power per unit of area *P*_m. The graphical interpretation of *P*_m is the area of the largest rectangle below the *J-V* curve; (*V*_{oc}*J*_{sc}) is the area if the curve were a true rectangle. From the definition of FF, it follows that *P*_m = FF (*V*_{oc}*J*_{sc}). The efficiency of a solar cell *g* is in fact the efficiency at maximum power delivery, so that *g* = *P*_m/*P*_{in}, where *P*_{in} is the incident light intensity. It is clear that any loss in FF will reduce the efficiency of the solar cell. One must note that *V*_{oc}, *J*_{sc} and FF are not the fitting parameters and do not depend on any model describing the solar cells.

Fig. 1 shows a comparison of the fill factor, FF as a function of excitation light intensity for both types of ZnO and SnO₂ substrate cells. Obviously, for the cell with SnO₂ substrate material, the FF is larger than that of the cell with ZnO substrate material. The FF decreases with the increasing light intensities for both types of cells. The small value of FF may be due to the high excitation intensity used. According to a model proposed by Crandal [12], for the weakly absorbed light, the shape of *J-V* curve is completely specified by electron and hole drift lengths.

Fig. 2 shows a comparison of *J-V* curves of devices in dark. As seen, the cell on SnO₂ gives almost an ideal diode *J-V* curve, i.e., the dark current almost constant at reverse bias. However, the dark current of cell on ZnO increases linearly with increasing reverse biases. It means that this cell has a large series contact resistance at the ZnO/p interface. This result prevents taking advantage of higher transmission through ZnO since the efficiency is lower due to lower *V*_{oc} and FF [13].

Fig. 3 shows a comparison of the short-circuit current, *J*_{sc} vs the open-circuit voltage, *V*_{oc}. The red irradiation intensities of 1–10 mW from the HeNe laser were used for this comparison. Obviously *J*_{sc}–*V*_{oc} characteristics exhibit two distinct regions in which the lines have different slopes for two-types of cells. Also there is a gap between *J*_{sc} and *V*_{oc} curves, and this gap increases at lower irradiations. However the *J*_{sc} for the cell on ZnO is larger than the other one at all irradiations levels. This result also confirms that the recombination increases at the TCO/p interface under lower irradiations as expected.

Fig. 4 shows a comparison of the quantum efficiency ratios, QE(–1.0 V)/QE(0 V) and QE(0.5 V)/QE(0 V), as a function of wavelength for two different cells on ZnO and SnO₂. As seen, the ratios at reverse bias are high and almost constant for both cells. It means that all photogenerated carriers were collected under reverse bias. However, the ratios at forward bias are low and quite different for higher wavelengths. At the short-wavelength side, the QE ratios are close to each other, but at longer-wave side, for instance at 700 nm the QE ratio of cell on SnO₂ is about 1.13 times

Table 1
Illuminated *J-V* results (AM1.5 global light from an Oriel simulator) for a-Si:H p-i-n solar cells deposited on ZnO and SnO₂. *R*_{oc} is the resistance at open circuit. Also shown are values of the QE integrated with the AM1.5 spectrum.

Sample	Substrate	<i>V</i> _{oc} (V)	<i>J</i> _{sc} (mA/cm ²)	FF (%)	<i>V</i> _{mp} (V)	<i>J</i> _{mp} (mA/cm ²)	<i>R</i> _{oc} (Ω cm ²)	Integrated QE (mA/cm ²)
4629-12	1 mm glass/ZnO (HRVD)	0.86	14.9	61.2	0.61	12.79	15.37	14.33
4631-12	1 mm glass/ZnO (HRVD)	0.85	14.89	61.0	0.61	12.61	12.00	14.20
4631-21	1 mm glass/ZnO (HRVD)	0.85	15.29	60.6	0.61	12.95	12.43	14.44
4631-22	3 mm glass/SnO ₂ (SLX)	0.87	14.55	67.0	0.66	12.86	6.99	13.31
4633-11	3 mm glass/SnO ₂ (LOF)	0.83	13.41	67.8	0.66	11.38	6.20	13.22
4633-22	3 mm glass/SnO ₂ (SLX)	0.85	15.16	71.3	0.66	13.90	4.62	14.36

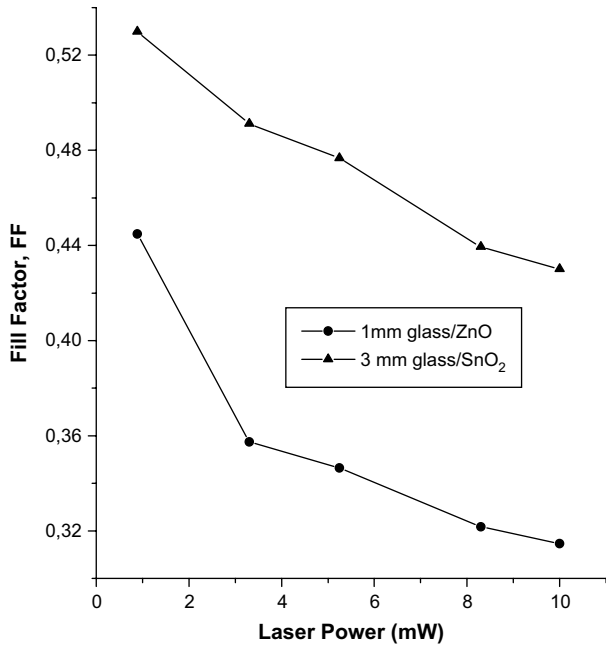


Fig. 1. A comparison of fill factor (FF) of a-Si:H p-i-n solar cells deposited on ZnO and SnO₂ substrates, with the red light intensity (632.8 nm). The lines are guide to the eyes.

larger than the other. This shows that the recombination loss is high in the cell on ZnO.

Photogenerated excess charge carriers can recombine via recombination centers and thus not contribute to the photocurrent. This is called recombination kinetics. It is a key feature when describing carrier transport in semiconductors because it strongly affects the electrical response of the semiconductor at all levels of external excitation. Measurement of photocurrent as a function of excitation light intensity, temperature, wavelength, modulation frequency and applied electric field gives invaluable information on

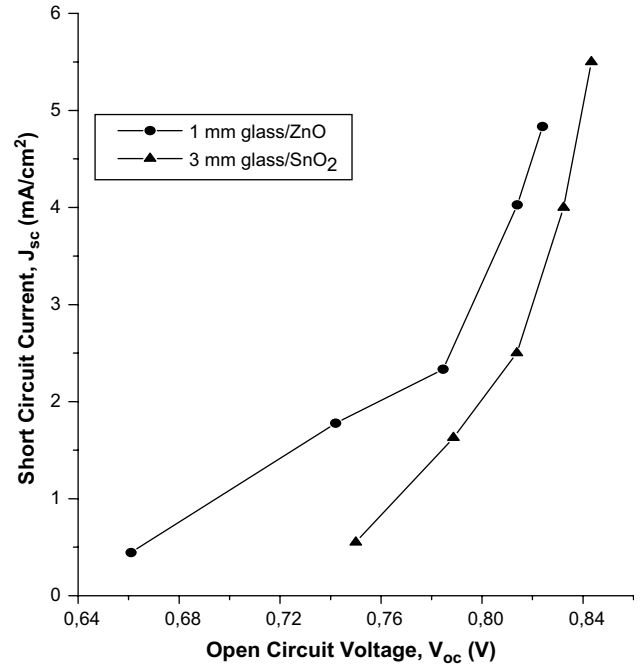


Fig. 3. A comparison of J_{sc} vs V_{oc} for the a-Si:H p-i-n solar cells deposited on ZnO and SnO₂. The lines are guide to the eyes.

the transport properties of photocarriers. The dependence of photocurrent I_{ph} on the photogeneration rate G (which is linearly proportional to the incident light intensity) is given by the power-law,

$$I_{ph} \propto G^v \quad (2)$$

It is differentially defined by

$$v = d[\ln(I_{ph})] / d[\ln(G)] \quad (3)$$

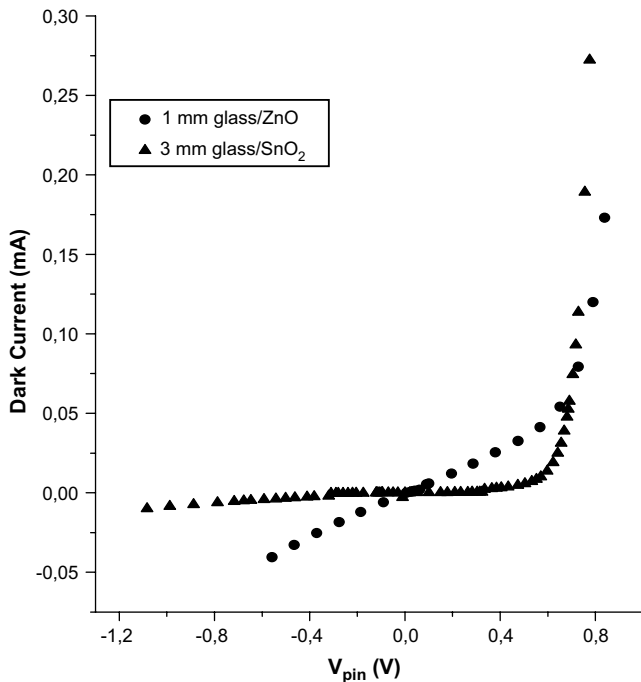


Fig. 2. A comparison of dark currents of a-Si:H p-i-n solar cells deposited on ZnO and SnO₂.

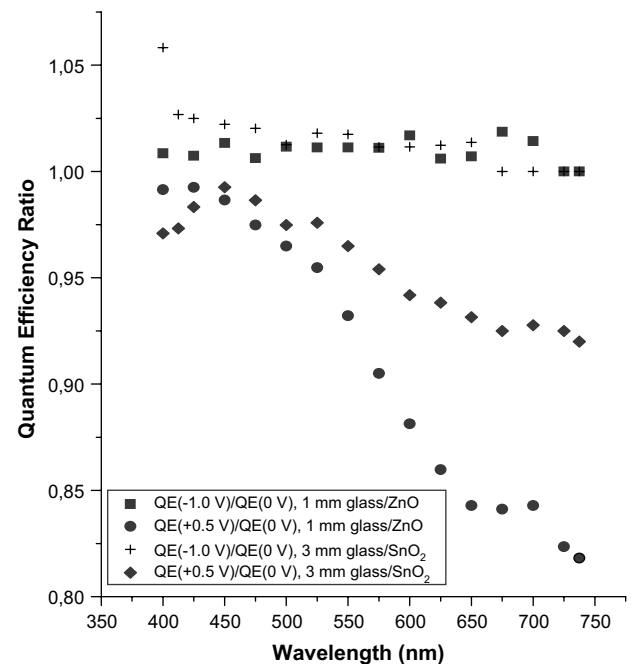


Fig. 4. A comparison of quantum efficiency ratios of a-Si:H p-i-n solar cells deposited on ZnO and SnO₂, as a function of wavelength at different bias conditions.

It is now well-known that the value of the exponent ν differs in various semiconductors and has quite complicated variations with temperature, photon frequency and light intensity [14]. It is common practice to attribute ν between 0.5 and 1.0 to a mixture of two limiting recombination mechanisms [15]: a monomolecular recombination type occurring through recombination centers (dangling bonds, such as), which would correspond to $\nu \sim 1.0$ and a bimolecular recombination process, in which the excess charge carriers recombine directly from the band tails ($\nu \sim 0.5$). An alternative model proposed by Rose [16] considers an exponential distribution of density of states (DOS) whose states are increasingly converted from trapping to recombination states as the light intensity increased. Different ν values between 0.5 and 1.0 are obtained from this model, which depend upon the slope of the DOS being swept by the steady state Fermi level, and on temperature. Recent numerical and analytical work on photoconductivity in a-Si:H by Bube [17] has

demonstrated that a relatively simple model for recombination via dangling bonds can produce superlinear photocurrent ($\nu > 1$) in undoped material. On the other hand, a sublinear characteristics with exponent ν as low as 0.4 has been observed by numerous groups [18–20]. However, a complete model covering the modulation frequency-dependence of ν has not emerged.

Fig. 5(a) and (b) shows a comparison of the exponent ν for both types of cells under DC and modulated light, as a function of applied voltage and modulation frequency respectively. In Fig. 5(a), there is a large change in DC exponent ν of the cell with SnO₂, while it is noisy for the cell with ZnO. The ν values of cell on SnO₂ are larger than those of cell on ZnO at all biases. For the cell on SnO₂, ν increases with increasing DC bias from -1.0 V to about 0.1 V, and then decreases.

Measurements of cells deposited on ZnO using two independent techniques have shown no signs of a rectifying barrier, and the contact resistance is comparable to that on SnO₂ [9]. Instead, an increase of the diode ideality factor is consistently observed for cells fabricated on ZnO, suggesting enhanced recombination losses. Our lower values of DC exponent ν of the cell on ZnO shown in Fig. 5(a) is consistent with this result.

In Fig. 5(b), values of the modulated exponent ν for the cell on ZnO are larger than those of the cell on SnO₂. For the cell on ZnO, the ν increases very fast with increasing modulation frequencies until about 2000 Hz, and it shows a peak at around 2500 Hz, and then it decreases sharply. In the cell on SnO₂, the ν follows almost the same trend as the cell on ZnO, but the increase in ν is slow below about 1500 Hz. There is also a big difference between DC and modulated exponent values of the cell on ZnO. It means that the modulated exponent is larger than DC exponent for the cell on ZnO. Unfortunately there is little work for this type of data in the literature. The large value of ν for the modulated light may be due to the contribution of electron-hole pairs originating from the deeper states (traps) nearer to ZnO-p/i layer. As the photocarrier concentration of ZnO layer increases with increasing frequency, the states near the bottom of the conduction band are filled and the probability of occupancy of states in conduction band becomes lower. Probability of occupancy of states in valence band, on the contrary,

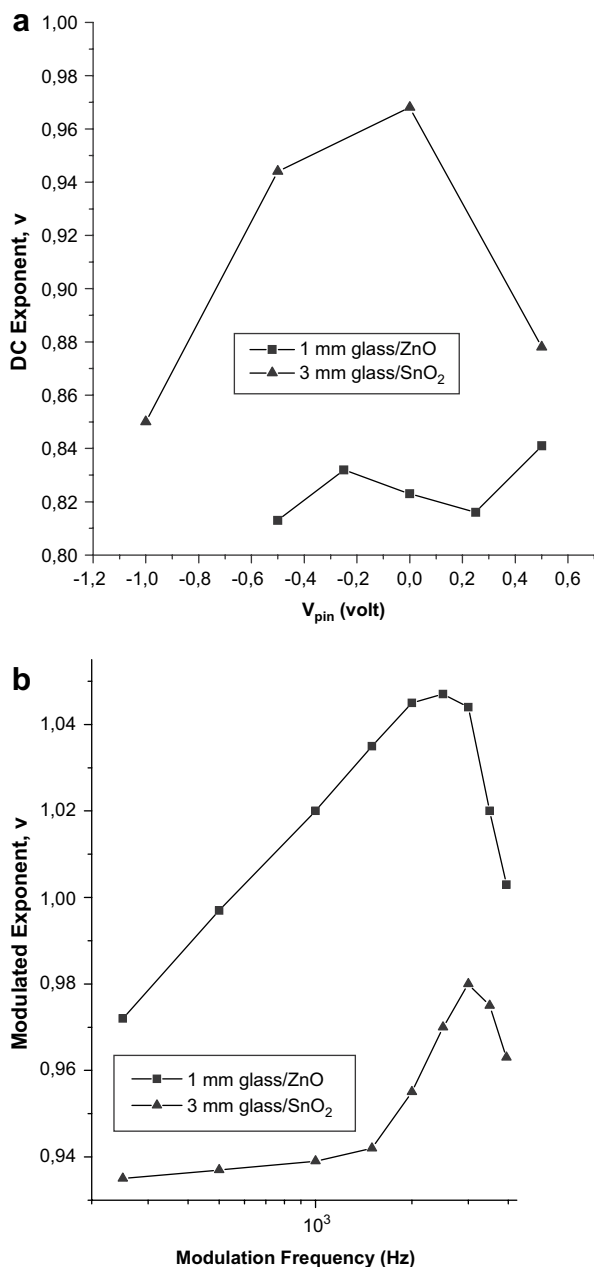


Fig. 5. A comparison of (a) DC and (b) AC (modulated) exponent ν ($I_{ph} \sim G^\nu$) in a-Si:H p-i-n solar cells deposited on ZnO and SnO₂. The lines are guide to the eyes.

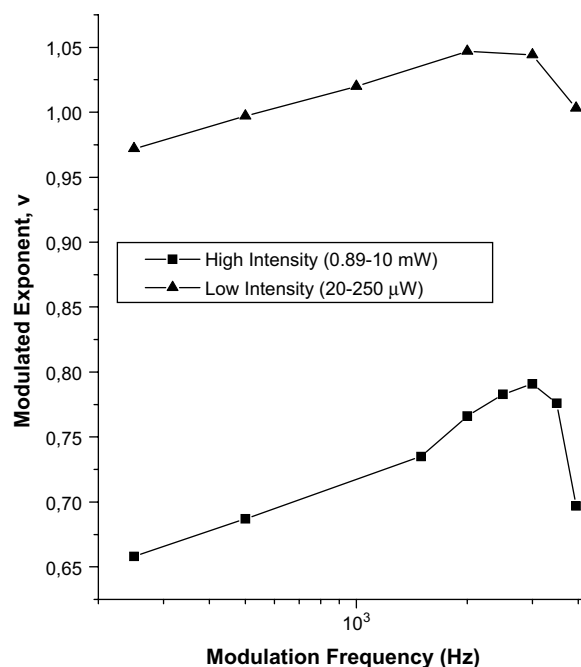


Fig. 6. A comparison of modulated exponent ν in a-Si:H p-i-n solar cell deposited on ZnO at high- and low-light intensities. The lines are guide to the eyes.

becomes higher, resulting in an increase of tunneling photocurrent of the minority carriers. As a result, the photocurrent, and thus the modulated exponent ν increases. However, we have no clear explanations for the decrease in ν on the higher modulation frequencies as shown in Fig. 5(b).

Fig. 6 shows the effects of high and low illumination levels on the modulated exponent ν of the cell with ZnO. As seen, the values of ν obtained at low intensities are quite larger due to recombination effects rather than drifting. At low intensities, it closes to ~ 1 , which corresponds to monomolecular recombination. Unfortunately, there are some recombination losses at high intensities. The value of exponent ν lies between about 0.65 and 0.80 for the cell on ZnO, indicating the presence of a continuous distribution of localized states in the TCO/p interface. However, both curves shown in Fig. 6 have a maximum at around 3000 Hz. Similar effects were also observed for the cell on SnO₂ substrate.

4. Conclusion

We examined the effects of two different substrate materials, i.e., ZnO and SnO₂ on a-Si:H p-i-n solar cells. We compared some cell performances, such as V_{oc} , J_{sc} , FF, QE; and some physical parameters, such as the exponent ν in the power-law relationship $I_{ph} \sim C^\nu$, as a function of the illumination intensity, the modulation frequency and bias voltages. Our a-Si:H p-i-n solar cells deposited on ZnO exhibit reduced FF, V_{oc} and ν (DC), but higher QE and modulated ν in comparison with SnO₂. Therefore it is well established that V_{oc} , FF, QE, ν (DC and modulated) are sensitive to the substrate material of ZnO and SnO₂ which have influences on the cell structure. They can be improved on a-Si:H p-i-n devices by the optimization of the TCO which acts as a window layer allowing most of the incident light to pass into the i-layer.

Our frequency-modulated results also act as a guide to the best experimental condition for comparing our data to the DC results.

Acknowledgements

This work was supported by TBAG-2212 (102T091) Contract of The Scientific and Technical Research Council of Turkey (TUBITAK).

References

- [1] Compaan AD. Photovoltaics: clean power for the 21st century. *Solar Energy Materials and Solar Cells* 2006;90:2170–80.
- [2] Hamakawa Y. Solar PV energy conversion and the 21st century's civilization. *Solar Energy Materials and Solar Cells* 2002;74:13–23.
- [3] Goetzberger A, Luther J, Willeke G. Solar cells: past, present, future. *Solar Energy Materials and Solar Cells* 2002;74:1–11.
- [4] Carlson DE. Monolithic amorphous silicon alloy solar modules. *Solar Energy Materials and Solar Cells* 2003;78:627–45.
- [5] Gren MA. Silicon photovoltaic modules: a brief history of the first 50 years. *Progress in Photovoltaics: Research and Application* 2005;13:447–55.
- [6] Schropp REI, Zeman M. In: Amorphous and microcrystalline silicon solar cells. London: Kluwer Academic; 1998. p. 69–109.
- [7] Manea E, Budianu E, Purica M, Cristea D, Cernica I, Muller R, et al. Optimization of front surface texturing processes for high-efficiency silicon solar cells. *Solar Energy Materials and Solar Cells* 2005;87:423–31.
- [8] Mahalingam T, Join VS, Raja M, Su YK, Sebastian PJ. Electrodeposition and characterization of transparent ZnO thin films. *Solar Energy Materials and Solar Cells* 2005;88:227–35.
- [9] Hegedus SS, Kaplan R, Ganguly G, Wood GS. Characterization of SnO₂/p and ZnO/p contact resistance and junction properties in a-Si p-i-n solar cells and modules. In: Proceedings of 28th IEEE PVSC; 2000. p. 728–31.
- [10] Hegedus SS, Albright S, Jeffrey F, McMahon TJ, Wideman S. Workshop report from the thin film photovoltaic symposium: substrates, contacts, and monolithic integration. *Progress in Photovoltaics: Research and Applications* 1997;5:365–70.
- [11] Hegedus SS, Kaplan R. Analysis of quantum efficiency and optical enhancement in amorphous Si p-i-n solar cells. *Progress in Photovoltaics: Research and Application* 2002;10:257–69.
- [12] Crandal RS. Modeling of thin film solar cells: uniform field approximation. *Journal of Applied Physics* 1983;54:7176–86.
- [13] Hegedus SS, Buchanan W, Liu X, Gordon R. Effect of textured tin oxide and zinc oxide substrates on the current generation in amorphous silicon solar cells. In: Proceedings of 25th IEEE PVSC; 1996. p. 1129–32.
- [14] Kaplan R. Comparative frequency-resolved photoconductivity studies of amorphous semiconductors. *Solar Energy Materials and Solar Cells* 2005;85:545–57.
- [15] Arene E, Baixeras J. Steady-state photoconductivity and recombination processes in sputtered hydrogenated amorphous silicon. *Physical Review B* 1984;30:2016–25.
- [16] Rose A. In: Concepts in photoconductivity and allied problems. NY: Krieger; 1978. p. 33–50.
- [17] Bube RH. A new mechanism for superlinear photoconductivity with relevance to amorphous silicon. *Journal of Applied Physics* 1993;74:5138–43.
- [18] Hack M, Guha S, Shur M. Photoconductivity and recombination in amorphous silicon alloys. *Physical Review B* 1984;30:6991–9.
- [19] Morgado E. Electron and hole $\mu\tau$ products in a-Si:H and the standard dangling bond model. *Journal of Non-Crystalline Solids* 1993;166:627–30.
- [20] Bube RH, Redfield D. Variation of photoconductivity with doping and optical degradation in hydrogenated amorphous silicon. *Journal of Applied Physics* 1989;66:3074–81.